

# EVIDENCE FROM THE MOTIONS OF OLD STARS THAT THE GALAXY COLLAPSED

O. J. EGGEN, D. LYNDEN-BELL,\* AND A. R. SANDAGE

Mount Wilson and Palomar Observatories

Carnegie Institution of Washington, California Institute of Technology

*Received May 17, 1962*

## ABSTRACT

The ( $U$ ,  $V$ ,  $W$ )-velocity vectors for 221 well-observed dwarf stars have been used to compute the eccentricities and angular momenta of the galactic orbits in a model galaxy. It is shown that the eccentricity and the observed ultraviolet excess are strongly correlated. The stars with the largest excess (i.e., lowest metal abundance) are invariably moving in highly elliptical orbits, whereas stars with little or no excess move in nearly circular orbits. Correlations also exist between the ultraviolet excess and the  $W$ -velocity. Finally, the excess and the angular momentum are correlated; stars with large ultraviolet excesses have small angular momenta.

These correlations are discussed in terms of the dynamics of a collapsing galaxy. The data require that the oldest stars were formed out of gas falling toward the galactic center in the radial direction and collapsing from the halo onto the plane. The collapse was very rapid and only a few times  $10^8$  years were required for the gas to attain circular orbits in equilibrium (i.e., gravitational attraction balanced by centrifugal acceleration). The scale of the collapse is tentatively estimated to be at least 10 in the radial direction and 25 in the  $Z$ -direction. The initial contraction must have begun near the time of formation of the first stars, some  $10^{10}$  years ago.

## I. INTRODUCTION

Beginning with Strömberg's early investigations of stellar motions, it has become increasingly clear that the galaxy contains many types of objects with a large range in kinematic properties. The most elementary classification by kinematic properties is that introduced by Oort (1926), who divided the stars into "low"- and "high"-velocity objects. The boundary value between the two groups was taken as the velocity where a marked asymmetry appears in stellar motions—63 km/sec. But the data accumulated in subsequent years show that the kinematic situation is more complex and much richer in detail than this simple division indicates. Various kinematic and spatial subsystems—such as young main-sequence stars in the galactic disk, old globular clusters, RR Lyrae variables, and extreme subdwarfs—form a near continuum from the very lowest to the very highest space velocities. Historically, the idea of a continuum in the velocity distribution was developed from the work of Strömberg and Oort by Vyssotsky and Williams (1948) through their extended investigations of proper motions, and by Schwarzschild (1952) who examined the possible origins of the high velocity stars.

It is now recognized that a study of these subsystems allows us partially to reconstruct the galactic past because the time required for stars in the galactic system to exchange their energies and momenta is very long compared with the age of the galaxy. Hence knowledge of the present energy and momenta of individual objects tells us something of the initial dynamic conditions under which they were formed. Furthermore, results from the theory of stellar evolution allow us to estimate the age of the stars in the various subgroups. This provides a method of investigating *changes* in the dynamic structure of the galaxy with time, as indicated by differences in the kinematic behavior of stars ordered in a time sequence. This paper attempts to show how far one can go in reconstructing the history of the galactic system by using observational data now available.

The results of Section IV show that remarkable correlations exist between the chemical composition of the individual stars, the eccentricity of their galactic orbits, their

\* Harkness Fellow on leave of absence from Clare College, Cambridge, England.

angular momenta, and the height they reach above the galactic plane. These correlations are interpreted by a sequence of events starting with the protogalaxy condensing out of a pregalactic medium, collapsing toward the fundamental plane, and shrinking in diameter until the present equilibrium state is reached where the gravitational attraction is just balanced by the centrifugal acceleration. Our data suggest that the oldest stars with the lowest abundance of the heavy elements must have been formed in the collapsing protogalaxy when its size was at least ten times its present diameter and, furthermore, that the collapse since first star formation was very rapid, taking place in only a few times  $10^8$  years.

The approach has been to analyze the orbital parameters of individual stars now passing through the solar neighborhood which have velocities relative to the sun distributed over the entire observed range of 0 to more than 300 km/sec. To this end we have used data from two catalogues (Eggen 1961, 1962) which contain computed values of the  $(U, V, W)$ -velocity vectors for a number of well-observed stars. The first catalogue contains the approximately 4000 stars (*a*) for which accurate pre- and post-1900 proper motions (Eggen 1961) from meridian observations are available, and (*b*) having radial-velocity determinations with an accidental error less than about 1.5 km/sec. The second catalogue contains all the stars for which the presently available data indicate a total space motion in excess of 100 km/sec. Although the proper-motion and radial-velocity data for stars in the second catalogue are of generally lower weight than the corresponding data in the first catalogue, the resulting uncertainty in the  $(U, V, W)$ -vectors is less than  $\pm 20$  km/sec in most cases. New, high-precision velocities obtained from coudé spectra with the 200-inch reflector of several known subdwarfs have kindly been made available by Greenstein before publication. Also, many new, high-velocity subdwarfs found by Sandage and Eggen in a recent photometric and radial-velocity search program are also included. The completeness of our second catalogue owes a great deal to Dr. A. Hunter and Dr. R. H. Stoy and their assistants at the Royal Greenwich and Cape Observatories for determining many photographic proper motions of faint stars.

## II. STELLAR DYNAMICS IN A STEADY POTENTIAL

### *a) The Potential Function*

In this subsection we treat the two-dimensional motion in the galactic plane for the case where the galaxy is in dynamical equilibrium (i.e., the potential is not a function of time). In two following subsections we treat the motion perpendicular to the plane and the case of a time-varying potential in a collapsing galaxy.

Cylindrical symmetry is assumed in all the cases discussed, so that the equations of motion can be integrated to give the energy and the angular momentum equations in  $(R, \phi)$  co-ordinates as<sup>1</sup>

$$\frac{\dot{R}^2}{2} + \frac{h^2}{2R^2} - \psi(R) = E_R, \quad (1)$$

$$R^2 \dot{\phi} = h, \quad (2)$$

where  $\psi(R)$  is the gravitational potential in the galactic plane. These can be put into the form

$$\phi = \frac{1}{2} \int \frac{hR^{-2}dR^2}{[2R^2(E_R + \psi) - h^2]^{1/2}}, \quad (3)$$

$$t = \frac{1}{2} \int \frac{dR^2}{[2R^2(E_R + \psi) - h^2]^{1/2}}, \quad (4)$$

<sup>1</sup> Throughout this paper, "energy" and "angular momentum" normally refer to energy per unit mass and angular momentum per unit mass about the galactic axis, respectively.

which are the parametric equations of the orbit. We now ask that all properties of the orbit be derived explicitly and eventually computed from the known  $(U, V)$ -velocity vectors of the individual stars. We therefore seek a general form for those potentials for which equations (3) and (4) may be integrated (parametrically) in terms of, say, trigonometric functions and which possess the boundary conditions

$$\begin{aligned}\psi &\rightarrow \frac{GM}{R} & \text{as } R \rightarrow \infty, \\ R\psi &\rightarrow \text{Const.} & \text{as } R \rightarrow 0,\end{aligned}$$

The second condition insures that there is, at most, a finite mass at  $R = 0$ . It can be shown that the most general potential with these properties for all values of  $E_R$  and  $h$  is

$$\psi = \frac{GM}{b + (R^2 + b^2)^{1/2}}, \quad (5)$$

where  $M$  is the total mass of the galaxy and  $b$  is a constant length which is zero for the Newtonian potential. If the gravitational attraction is everywhere balanced by the centrifugal acceleration, the circular velocity at any  $R$  is given by equation (5) as

$$V = \frac{(GM)^{1/2}R}{[b + (R^2 + b^2)^{1/2}](R^2 + b^2)^{1/4}}. \quad (6)$$

To evaluate  $b$ , we fit equation (6) to the observed Oort constants,  $A$  and  $B$ , at  $R_\odot$ . Put

$$q = \left[ \left( \frac{R_\odot}{b} \right)^2 + 1 \right]^{1/2}, \quad (7)$$

then

$$-\frac{A+B}{A-B} = \left( \frac{R}{V} \frac{dV}{dR} \right)_\odot = \frac{1 + 2q - q^2}{2q^2} \quad (8)$$

by equation (6). Taking  $A = 15$  km/sec/kpc and  $B = -10$  km/sec/kpc, we obtain  $q = 3.77$ , and, therefore, from equation (7)  $R_\odot = 3.65b$ . The total mass,  $M$ , may now be found from equation (6), provided that we know  $R_\odot$  and  $V_\odot$ . For  $R_\odot = 10$  kpc and  $V_\odot = 250$  km/sec, we find  $b = 2.74$  kpc,  $(GM/b)^{1/2} = 635$  km/sec, and  $M = 2.4 \times 10^{11} \odot$ . A graph of equation (6) with these values is plotted in Figure 1 with the Leiden 21-cm observations, corrected to the above values of  $A$ ,  $B$ , and  $R_\odot$ , shown for comparison.

#### b) Properties of Orbits in This Potential

In working out equations (3) and (4) of the orbit, it is convenient to define a dimensionless potential  $\Psi$  to use as a variable in place of  $R$ :

$$\Psi = \frac{\psi b}{GM} = \frac{1}{1 + [(R^2/b^2) + 1]^{1/2}}. \quad (9)$$

Further, the closed integrals of equations (3) and (4) can be neatly expressed by using auxiliary quantities defined by

$$\alpha^2 = 1 + 4bGMh^{-2}, \quad \beta^2 = \gamma^2 + 2E_R b^2 h^{-2} \alpha^{-2}, \quad \gamma = (GM - 2E_R b) b h^{-2} \alpha^{-2}. \quad (10)$$

Note the identity

$$\alpha^{-2} = 1 - 4[\gamma - (\gamma^2 - \beta^2)] \equiv (2\gamma - 1)^2 - 4\beta^2. \quad (11)$$

Equations (3) and (4) then become

$$\phi = a^{-1} \int \frac{(1 - \Psi) d\Psi}{(1 - 2\Psi)[\beta^2 - (\Psi - \gamma)^2]^{1/2}}, \quad (12)$$

$$t = \frac{b^2}{a h} \int \frac{(1 - \Psi) d\Psi}{\Psi^2 [\beta^2 - (\Psi - \gamma)^2]^{1/2}}. \quad (13)$$

The perigalacticum and apogalacticum of the orbit are reached at the singularities  $\Psi = \gamma \pm \beta$ , which occur where  $\dot{R}$ ,  $dR/d\phi = 0$  or, equally,  $\dot{\Psi}$ ,  $d\Psi/d\phi = 0$ . At apogalacticum,  $\Psi = \gamma - \beta$ , or

$$R_1 = \frac{b}{\gamma - \beta} [1 - 2(\gamma - \beta)]^{1/2}. \quad (14)$$

At perigalacticum,  $\Psi = \gamma + \beta$ , or

$$R_2 = \frac{b}{\gamma + \beta} [1 - 2(\gamma + \beta)]^{1/2}, \quad (15)$$

where we have used  $R = b\Psi^{-1}(1 - 2\Psi)^{1/2}$ , derived from equation (9).

The eccentricity of the orbit is arbitrarily defined by

$$e = \frac{R_1 - R_2}{R_1 + R_2}, \quad (16)$$

which is formally correct for a focal ellipse; but, since orbits with our potential are not closed, the definition of the eccentricity is arbitrary (but see Sec. III on the adiabatic invariant for a time-dependent potential).

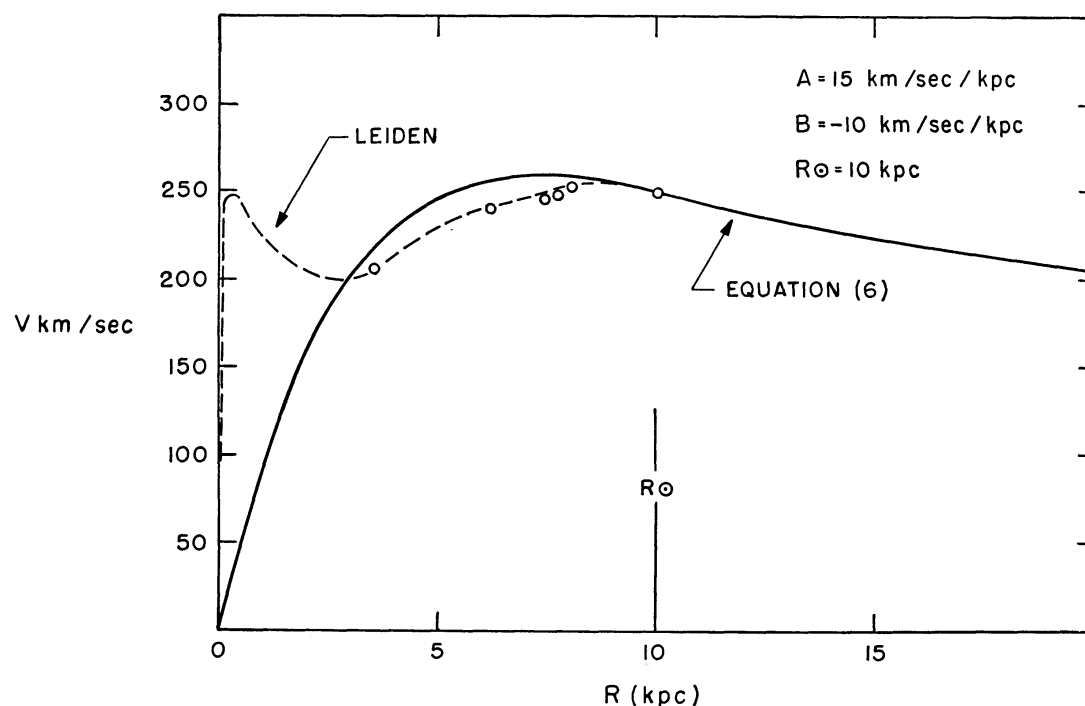


FIG. 1.—The circular velocity,  $V$ , in km/sec as a function of the distance,  $R$ , in kiloparsecs from the galactic center. The continuous curve is obtained from equation (6) with  $b = 2.74$  kpc and  $M = 2.4 \times 10^{11} M_{\odot}$ . The 21-cm observations from Leiden are indicated by open circles. The dashed part of the curve comes from Rougoor and Oort (1960).

Equations (12) and (13) may be explicitly integrated to give

$$\phi = \frac{1}{2a} \sin^{-1} \left[ \frac{\Psi - \gamma}{\beta} \right] + \tan^{-1} \{ a [ \tau (1 - 2\gamma) - 2\beta ] \}, \quad (17)$$

$$t = \frac{2b^2}{ah} \left\{ \frac{\gamma - (\gamma^2 - \beta^2)}{(\gamma^2 - \beta^2)^{3/2}} \tan^{-1} \left[ \frac{\tau + \gamma}{(\gamma^2 + \beta^2)^{1/2}} \right] + \frac{\beta(\gamma + \tau\beta)}{\gamma(\gamma^2 - \beta^2)[\gamma(1 + \tau^2) + 2\beta\tau]} \right\}, \quad (18)$$

where

$$\tau = \tan \left[ \frac{1}{2} \sin^{-1} \left( \Psi - \frac{\gamma}{\beta} \right) \right] = \frac{\beta \pm [\beta^2 + (\Psi - \gamma)^2]^{1/2}}{\Psi - \gamma}.$$

Equations (17) and (18) have been used in the present study only to draw a few orbits for representative stars; for other purposes, much simpler formulae may be derived from equations (17), (18), (9), (10), and (11). For example, the angle swept out between successive apogalactica is

$$\Phi = \pi \left( \frac{1}{a} + 1 \right); \quad (19)$$

the time between successive apogalactica is

$$T = 2\pi GM(-2E_R)^{-3/2}; \quad (20)$$

and the mean period around the galaxy is

$$P = \frac{2\pi T}{\Phi}. \quad (21)$$

The orbits of four stars, computed from equations (10), (17), and (18), are shown in Figures 2 and 3.

### c) *The Effect of Motion Perpendicular to the Galactic Plane*

Certain potentials have exact third integrals of the motion. The potential  $\psi(R) + \psi_1(Z)$  gives completely independent motions in the plane and at right angles to it, with each energy separately conserved. The potential  $\psi(r) + r^{-2}\psi_1(\theta)$ , where  $(r, \theta, \phi)$  are spherical polar co-ordinates, keeps  $\frac{1}{2}|\omega|^2 - \psi_1(\theta)$  constant throughout the motion where  $\omega$  is the total angular momentum vector. For such special potentials the complete orbits may be found in terms of quadratures. A list of such special potentials and their integrals is given by Lynden-Bell (1962). Probably none of these are exactly realized in actual galaxies, and we must fit such a special potential to the galaxy and hope the discrepancies can be made small (but not negligible).

We obtain a crude estimate of the effects of neglecting the  $Z$ -motion (i.e., motion perpendicular to the plane) in the following way. We suppose that while the star traverses one semiperiod in its  $Z$ -motion, it moves so little in  $R$  that the potential may be taken as separable. For nearly circular orbits the semiperiod in  $R$  is three times the semiperiod in  $Z$ , while the ratio increases for non-circular orbits. Thus our approximation of small change in  $R$  during the semiperiod in  $Z$  is better than that of complete separability throughout the orbit. With these assumptions, the adiabatic invariant,  $\oint p_Z dZ$ , is conserved. The symmetry about  $Z = 0$  allows us to evaluate the invariant over a semiperiod. Thus  $\oint \dot{Z} dZ = \text{constant}$ . From the energy equation we find  $\dot{Z}$  and, therefore,

$$\oint \{ 2[E + \psi(R, Z)] - h^2 R^{-2} - \dot{R}^2 \}^{1/2} dZ = \text{Const.} \quad (22)$$

This is an approximate third integral. To evaluate it explicitly, let us first assume that  $\psi$  is of the form  $\psi = \psi(R) - C(R)\psi_1(Z)$ , where  $\psi_1(Z) = Z^2 + O(Z^4)$  near  $Z = 0$ . Then Poisson's equation yields

$$C(R) \simeq 2\pi G\rho(R, 0). \quad (23)$$

Let us also define  $E_R = \frac{1}{2}(\dot{R}^2 + h^2 R^{-2}) - \psi(R)$ , and  $E_Z = E - E_R$ . Note that these are no longer constants of the motion, but from their definitions they are explicitly independent of  $Z$  and are to be considered so when the integration in equation (22) is performed. We may write equation (22) as

$$\mathcal{J} \{2[E_Z - C(R)\psi_1(Z)]\}^{1/2} = \text{Const.}$$

If the  $Z$ -motion is of small amplitude,  $\psi_1$  may be approximated by  $Z^2$ , and we have

$$\pi\sqrt{(2)E_Z C^{-1/2}} = \text{Const.}, \quad (24)$$

whence  $E_Z = \text{Const.} \sqrt{\rho(R, 0)}$ . Evaluating the constant at  $R_\odot$ , we have

$$E_Z = E_{Z\odot} \sqrt{\frac{\rho(R)}{\rho(R_\odot)}}, \quad (25)$$

where the densities are to be evaluated on the galactic plane. The energy equation for the  $R$ -motion may be deduced from the total energy equation and equation (25); it is

$$\frac{h^2}{2R^2} + \frac{\dot{R}^2}{2} - \psi(R) = E_R = E - E_Z = E_{R\odot} + E_{Z\odot} \left[ 1 - \sqrt{\frac{\rho(R)}{\rho(R_\odot)}} \right], \quad (26)$$

or

$$\frac{h^2}{2R^2} + \frac{\dot{R}^2}{2} - \psi(R) = E_{R\odot},$$

where

$$\psi = \psi(R) - E_{Z\odot} \left[ \sqrt{\frac{\rho(R)}{\rho(R_\odot)}} - 1 \right].$$

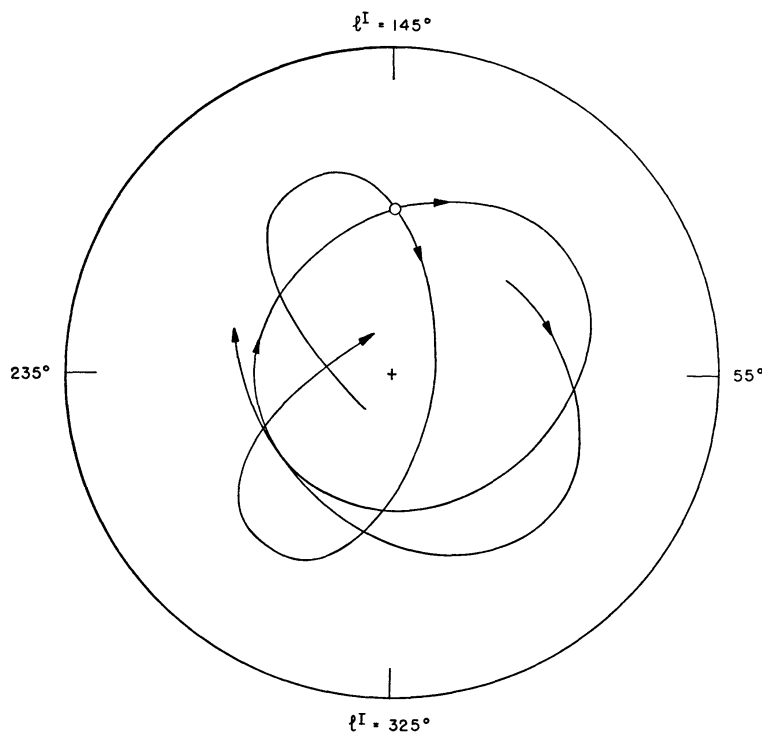


FIG. 2.—Segments of the galactic orbits for two of the program stars. The more circular orbit is for HD 117635 with an ultraviolet excess of  $\delta = +0^m05$ . The more elliptical orbit is for HD 11980 with  $\delta = +0^m17$ . Both orbits pass through the solar neighborhood, which is designated by a circle on the  $l = 145^\circ$  axis at a distance of 10 kpc from the galactic center. The galactic center is shown as a cross. The outer circle has a radius of 20 kpc.



We now see from equation (26) that the actual motion in  $R$  is as though the potential in the galactic plane was not  $\psi(R)$  but  $\tilde{\psi}(R)$ . If  $\rho(R, 0)$  decreases with  $R$ , this  $E_Z\odot$ -dependent addition to the potential increases both apogalacticum and perigalacticum distance. The effect is small for  $E_Z\odot$  small compared with  $E_R\odot$  and has been neglected in the computations in Section IV. Even when the neglect is not valid, the planar "eccentricity" as defined by equations (14), (15), and (16) still classifies orbits into "near circular" and "near rectilinear" groups.

### III. DYNAMICS IN A CONTRACTING GALAXY

Later we will have to consider times before the potential field of the galaxy was independent of time. It is important to know what properties of a stellar orbit are preserved throughout its history and how other properties are changed by changes in the galactic

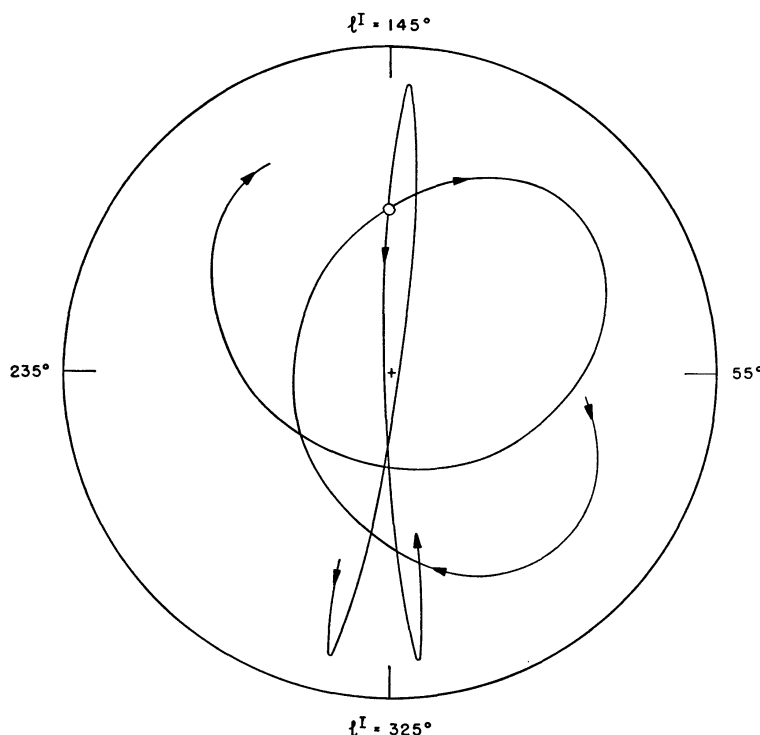


FIG. 3.—Same as Fig. 2. The more circular orbit is for HD 29587 with  $\delta = +0^m13$ . The more elliptical orbit is for Ross 106 with  $\delta = +0^m26$ . The orbit for Ross 106 is retrograde.

field. Since at earlier times much of the galaxy was gas, it is equally important to discuss some of the properties of the gas dynamics. We shall make two assumptions: (1) the gravitational potential of the galaxy is axially symmetrical at all times, and (2) masses whose angular momenta (about the galactic axis) are significantly different from one another do not exchange angular momenta through pressure gradients or magnetism. Assumption 1 is really the assumption that our Galaxy was never a barred spiral. Assumption 2 is probably correct if the scale of any turbulence was always much smaller than the size of the galaxy. We assume the truth of both assumptions for all times since the first stars in our Galaxy were formed.

Under these circumstances the main forces on the material will always have occurred in planes containing the galactic axis, and *each element of matter will have conserved its angular momentum*. In practice, the distribution of angular momentum with mass, as

deduced from observations of the Andromeda Nebula, agrees quite well with Mestel's (1961) suggestion that it might be the same as that for a uniform and uniformly rotating sphere. This lends some support to the hypothesis of detailed conservation of angular momentum for each element of fluid ever since the galaxy was a cloud of gas.

Cosmic gas masses suffer inelastic collisions with their neighbors and radiate the heat generated, whereas stars do not collide with anything. (However, in a time-dependent potential, stars do not conserve their energy of motion.) In a steady galaxy, knowledge of the gravitational potential, the angular momentum of a star, and the eccentricity of its orbit determine the planar orbit completely. We have argued that the angular momentum is conserved in spite of changes in the galaxy, but we still must determine the change of the eccentricity. We consider two cases: (1) potentials changing slowly, with little change during one galactic rotation, and (2) potentials changing rapidly, with considerable change in one rotation. For the purpose of obtaining a rough estimate of the way in which the eccentricity changes with time, we shall assume that the potential in the galactic plane is always of the form given by equation (5) but that  $b$  is a function of time, because we are assuming that the mass distribution is changing and becoming more concentrated toward the center. In case 1 we again have an adiabatic invariant (i.e., a quantity that is conserved, provided that the changes are slow):

$$\oint P_R dR = \text{Const.} \quad (27)$$

For a planet circulating about a sun of slowly changing mass ( $b = 0$ ), this leads to a constant eccentricity of the planetary orbit. For  $b \neq 0$ , we find from complicated algebra and equation (27) that

$$\left[ (h^2 + 4bGM)^{1/2} + h - \frac{2GM}{(-2E_R)^{1/2}} \right] = \text{Const.}, \quad (28)$$

which vanishes for circular orbits, as equation (27) clearly requires.

For  $h^2 \gg 4bGM$ , equation (28) gives the Newtonian case of constant eccentricity. This suggests a connection with the eccentricity in the general case. In fact, if we define an invariant eccentricity,  $e^*$ , by

$$1 - (e^*)^2 = \left[ \frac{1}{2} - \left( \frac{1}{4} + \frac{bGM}{h^2} \right)^{1/2} + \frac{GM}{(-2E_R h^2)^{1/2}} \right]^{-2}, \quad (29)$$

then (a)  $e^*$  is an adiabatic invariant, in that it does not change if there is little change in the potential during one galactic period; (b)  $e^* = 0$  for circular orbits; (c)  $e^* = 1$  for straight-line orbits ( $h = 0$ ); and (d)  $e^* = e$  for  $h^2 \gg 4bGM$ .

The eccentricity defined earlier by equation (16) has no simple mathematical connection with  $e^*$ , but in practice their values do not differ by more than about 0.1. Therefore, although the correlations discussed in the next section were found for  $e$  and not for  $e^*$ , the correlation diagrams would show no significant change if  $e^*$  were used instead. In the remainder of this paper we shall regard the eccentricity,  $e$ , as the adiabatic invariant.

The adiabatic invariant of the  $Z$ -motion (eqs. [22] and [24]) has already been discussed. We need only remark that it is still invariant when the galaxy changes slowly.

In case 2, of a rapidly changing potential, we are led by simple examples to the belief that the eccentricity will, in general, increase when the mass concentration increases in a time that is short compared with the galactic period. One such example is that if, in the earth-sun system, the sun's mass was instantaneously increased by a factor of 2, the eccentricity of the earth's orbit would be increased from zero to  $\frac{1}{2}$ . Following this analogy, we shall assume that the eccentricity of a star's galactic orbit will, on the average, be increased when the mass concentration of the galaxy is increased. We recognize, however, that the effect of this sudden increase in mass concentration on stars near their perigalacticum will be to decrease the orbital eccentricity, but, because a relatively



short time is spent by each star in this part of its orbit, our assumption still holds in the average. However, the rate at which the mass becomes concentrated in the galaxy does not influence the conclusions which lead to our adopted model in Section V.

For the  $Z$ -motions we find that the velocity with which the star crosses the galactic plane will either be increased or remain the same when the density in the plane is increased, and the height the star reaches above the plane will, of course, be decreased in such circumstances.

The conclusions reached in Sections II and III can be summarized in the following way:

1. If we imagine the protogalaxy to be divided into rings according to the angular momentum per unit mass of the material in each ring, then a measure of the present angular momentum of any star formed from that material will permit the identification of the ring in which it originated.
2. If the mass concentration in the galaxy changed in a time that is long compared with a galactic period, the eccentricity of the galactic orbits and the value of  $E_Z[\rho(R, 0)]^{-1/2}$  for each orbit will be the same now as it was when the star was formed out of the gas.
3. If the mass concentration changed rapidly, compared with a galactic period, the present orbits will, on the average, be more eccentric than the orbits of the gas clouds from which the stars were formed. The energy in the  $Z$ -motion will be bounded between that which would give the greatest height above the galactic plane reached by the parent cloud and that which would give the same velocity as that attained by the parent cloud when it crossed the galactic plane.

#### IV. CORRELATIONS AMONG THE OBSERVED DATA

Parameters of the galactic orbits for 221 stars have been computed by means of equations (14), (15), and (16). Because all these objects, of which 108 are from the first catalogue (Eggen 1961) and 113 from the second (Eggen 1962), are within a few hundred parsecs of the sun, the energy and angular momentum for each orbit can be obtained from equations (1), (2), and (5) by putting  $R = 10$  kpc, as follows:

$$E_R = \frac{1}{2}[U'^2 + (V' + 250)^2] - 8.43 \times 10^4 \text{ km}^2/\text{sec}^2. \quad (30)$$

The velocity vectors ( $U'$ ,  $V'$ ) are directed away from the galactic center and toward the direction of galactic rotation, respectively. These vectors are relative to the "local standard of rest," which is defined by a solar motion,  $(U', V')_{\odot} = (-10, +15)$ . All the stars discussed here are believed, from spectroscopic or trigonometric parallax data, to be dwarfs, and the distances were obtained by force-fitting to the Hyades main sequence after the appropriate blanketing corrections had been made to the observed values of  $B - V$  (Sandage and Eggen 1959).

##### a) Correlation of Eccentricity, $e$ , and Ultraviolet Excess, $\delta(U - B)$

Analysis of the data in Roman's (1955) catalogue of high-velocity stars shows the remarkable result that stars with total space velocities greater than about 200 km/sec invariably have large ultraviolet excesses compared with the stars in the Hyades cluster (Sandage and Eggen 1959). Moreover, the ultraviolet excess appears to increase monotonically with the total space velocity (Roman 1955). The implication that a correlation must therefore exist between the orbital eccentricity,  $e$ , and the ultraviolet excess was the initial motivation for the present work. Figure 4 shows the correlation obtained from our data; the closed circles represent stars from the first catalogue and the open circles those in the second, high-velocity catalogue. Apparently the stars now in the vicinity of the sun, as represented by those in the two catalogues discussed, with large values of the ultraviolet excess (i.e., low abundance of the heavy elements) have very eccentric

orbits, whereas all those with little or no excess have nearly circular orbits. To assess the reality of Figure 4, it is important to know to what extent the stars in these catalogues are representative of the population in the solar vicinity.

Stars with nearly circular orbits have velocities that differ little from that of the "local standard of rest." Although radial-velocity determinations have been made for all stars to visual magnitude 5.5, observations of fainter stars, with the exception of a few special classes of high-luminosity objects, have usually been confined to those with appreciable ( $>0.1/\text{yr}$ ) proper motion. This means that there is some bias in our observational data

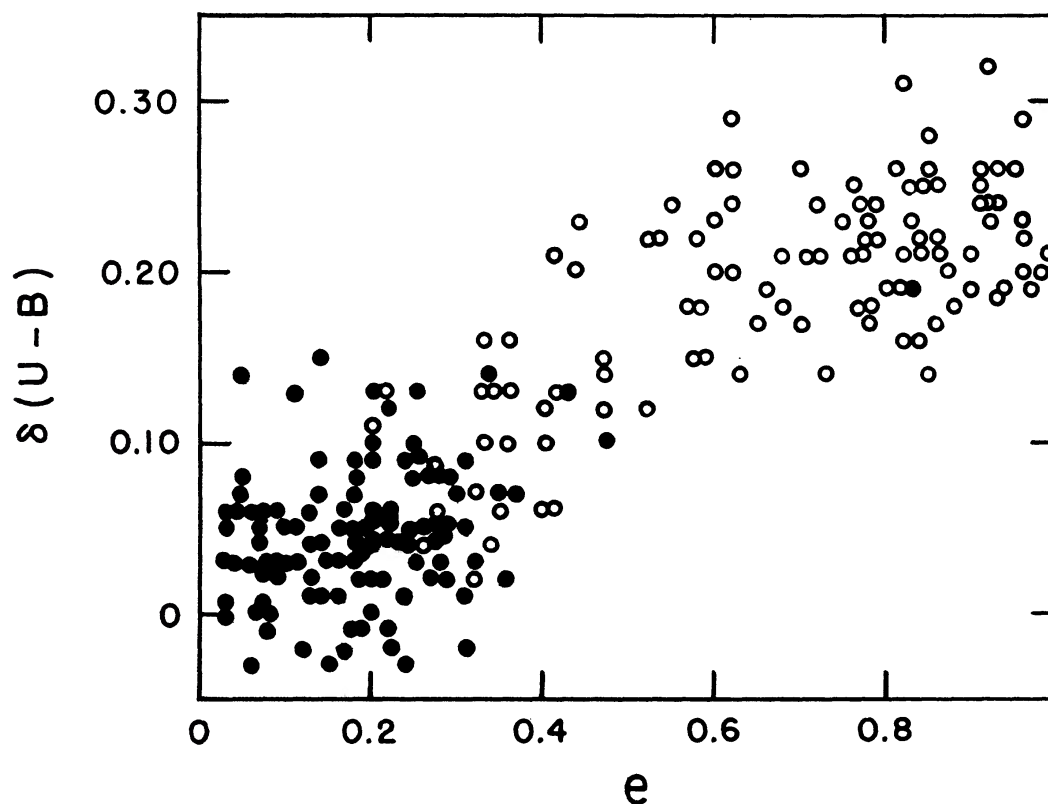


FIG. 4.—The correlation between the ultraviolet excess,  $\delta(U - B)$ , and the orbital eccentricity,  $e$ , for our sample of 221 stars. The filled and open circles represent stars from our first and second catalogues, respectively.

against stars with nearly circular orbits. However, in the photometry of stars for which velocities are available there is no observational bias in the ultraviolet excesses obtained, and it is therefore significant that the stars in the range  $0 \leq e < 0.3$  of Figure 4 *all* have small excesses. We conclude, therefore, that the lack of stars in the upper left section of Figure 4 is probably not a result of observational selection.

Although a few recently discovered subdwarfs had initially been put on radial-velocity programs because photometric observations indicated the presence of an ultraviolet excess, the vast majority of stars in our catalogue of high-velocity stars were discovered before accurate photometry was available, so that no observational bias for large excesses is present and therefore the lack of stars in the lower right section of Figure 4 must be real. However, the relative scarcity of stars in the range  $0.3 < e < 0.6$  in Figure 4 probably arises from the neglect of stars with intermediate velocity.

We now suggest that a correlation of  $e$  with  $\delta(U - B)$  is a correlation of  $e$  with age,

by the following argument. The subdwarfs in the general field, with ultraviolet excesses greater than about  $0^m2$ , can be identified with the main-sequence stars of globular clusters. This identification, which is made on the similarity of both the ultraviolet excesses and the kinematic parameters (high space motion and an isotropic distribution of velocity vectors), then indicates that these subdwarfs are as old as the globular clusters themselves—near  $10^{10}$  years. On the other hand, a variety of well-known arguments makes it clear that stars with little or no ultraviolet excess are relatively young. Although there are several indications that the gradual enrichment by heavy elements of the prestellar medium has been non-uniform in space, we shall adopt the working hypothesis that correlations with the ultraviolet excess and therefore with the metal abundance of the stars concerned are correlations with time. (We recognize, however, that the ultraviolet excess, as such, is undoubtedly non-linear with time.) Figure 4 then gives the remarkable result that  $e$  is correlated with time.

While the regression of ultraviolet excess on eccentricity shown in Figure 4 is believed to be new, it is implicitly contained in several previous studies of high-velocity stars. Lohmann (1948) discussed the orbits of 59 subdwarfs and found that the orbital eccentricities were all very high. A similar result was obtained by Roman (1954). Newkirk (1952) found the orbits of 50 RR Lyrae variables to be highly eccentric, and Yasuda (1961) reached the same conclusion from a discussion of several high-velocity stars. Finally, von Hoerner (1955), and, later Kinman (1959*b*) concluded from radial-velocity data that the halo globular clusters are probably moving in nearly rectilinear orbits.

*b) Correlation of the Velocity Perpendicular to the Plane and the Ultraviolet Excess*

The extreme subdwarfs show an almost isotropic velocity distribution (e.g., Fricke 1950), which identifies them as halo objects. The absolute values of the velocity perpendicular to the galactic plane,  $|W|$ , of the stars in our two catalogues are plotted against the ultraviolet excess in Figure 5. As in Figure 4, the filled and open circles represent, respectively, stars from our first and second catalogues. Because all these stars are within a few hundred parsecs of the sun, the value of  $|W|$  is essentially that which the star has when it crosses the galactic plane. In the absence of energy dissipation, the greater the value of  $|W|$ , the higher will be the maximum distance,  $Z(\text{Max.})$ , the star can eventually reach above or below the plane. The values of  $Z(\text{Max.})$  given on the right-hand side of Figure 5 were computed for us by D. Jones from a model for the acceleration in the  $Z$ -direction that is based on Woolley's (1958) results for stars near the plane and extended to very high  $Z$ -distances in a manner similar to that used by Oort and van Worekom (1941). Figure 5 shows that stars with the highest values of  $|W|$  can travel to heights greater than 10000 parsecs, putting them into the realm of the halo globular clusters. This is convincing evidence that the extreme subdwarfs—that is, subdwarfs with ultraviolet excesses greater than  $0^m2$ —can be identified with the main-sequence stars of globular clusters.

It is clear from Figure 5 (see also Wallerstein 1962, Fig. 19) that the mean height reached by stars is correlated with  $\delta(U - B)$  and therefore, presumably, with the epoch of formation. This result is in agreement with that obtained from independent data for related types of objects such as the globular clusters and field RR Lyrae variables. Kinman (1959*a*), following and extending Mayall's (1946) and Morgan's (1956) spectral classification work, has shown that grouping globular clusters according to the strength of the metal lines in their spectra also groups them according to their mean values of  $Z$ —weak-line clusters forming a distended halo reaching heights of at least 10000 parsecs; the intermediate-line strengths showing in clusters with a mean  $Z$  of about 4000 parsecs; and the strong-lined clusters located near the plane. Similar results were found by Preston (1959) for the RR Lyrae variables in the general field. The variables with  $\Delta S = 10$  (i.e., with greatly weakened metal lines) are generally found either far from the plane or with large values of  $|W|$  when they are near the plane; those with intermediate metal-line

strengths ( $\Delta S \approx 5$ ) are at intermediate heights; and the strong-line stars ( $\Delta S < 3$ ) lie near the plane. Furthermore, the large solar motion obtained from analysis of the radial velocities of the weak-line RR Lyrae variables implies that the orbits of these objects are highly eccentric, whereas the solar motion relative to the strong-lined variables is small and the orbits, therefore, nearly circular.

#### V. INTERPRETATION

If the ultraviolet excess is, in general, correlated with the ages of the stars, then *Figure 5 suggests that the oldest objects were formed at almost any height above the galactic plane,*

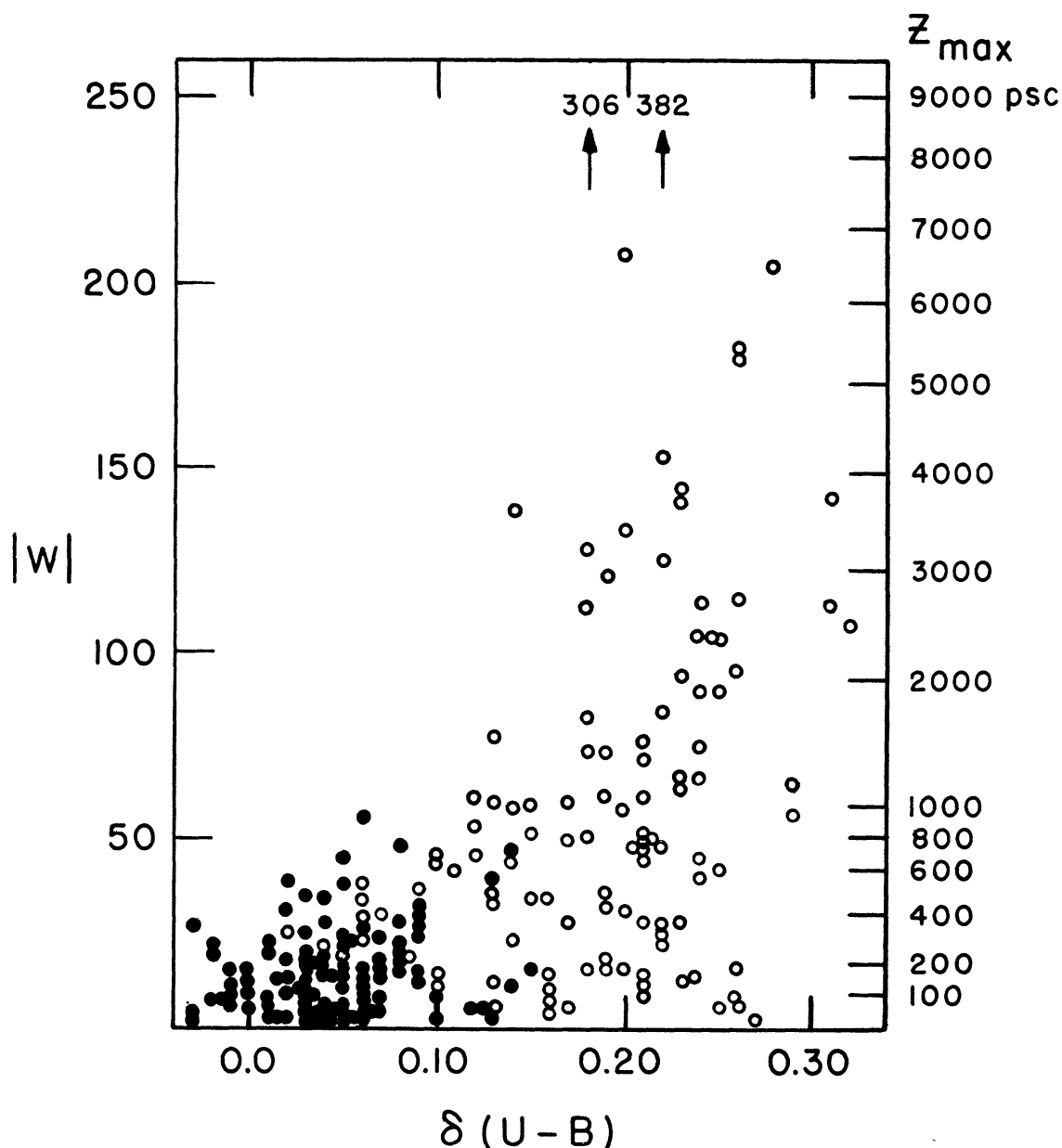


FIG 5 —The correlation between the  $W$ -velocity, perpendicular to the galactic plane, and the ultraviolet excess for the 221 stars in our sample. The filled and open circles represent the stars in our first and second catalogues, respectively.



whereas the youngest were formed very near the plane. This follows if the source of the  $Z$ -component of the kinetic energy is assumed to be the potential field through which the material falls onto the plane from its original great height. Although the relatively high  $Z$ -distances of a very few supergiants and the high  $W$ -motions known to exist for a few "runaway" B-type stars may have resulted from the application of some energy source in the plane—such as through a supernova explosion (Blaauw 1961)—there is little doubt that the vast majority of stars in Figure 5 did not receive their  $W$ -velocities in this way.

It appears, therefore, that a collapse of the galaxy into a disk, either after or during the formation of the oldest stars, is required to explain Figure 5. The well-defined upper envelope in the figure is then taken as the maximum height where star formation could take place at the epochs corresponding to given values of  $\delta(U - B)$ . The maximum value of  $Z$  for stars with  $\delta(U - B) > 0^m.2$  is about 10000 parsecs, whereas  $Z(\text{Max.})$  for stars with  $\delta(U - B) < 0^m.1$  is about 400 parsecs. This last value may be taken as the half-width of the galactic plane in which the recent (within about  $10^9$  years) star formation has taken place. The extent in the  $Z$ -direction of the material out of which stars were formed has therefore changed by a factor of at least 25—from 10000 to 400 parsecs—from the time of the earliest star formation some  $10^{10}$  years ago. Consideration of the collapse, in the radial direction, of the disk itself, which is discussed below, suggests that the process was very rapid and consumed a time span of not more than a few times  $10^8$  years.

Interpretation of Figure 4 is not so straightforward. It is necessary to understand why the first stars formed in the galaxy are now moving in nearly rectilinear orbits while stars formed more recently are moving in more circular orbits. An obvious suggestion might be that the galaxy was originally a gravitating sphere in equilibrium, supported everywhere by the appropriate, spherically symmetric pressure gradient. If stars condensed out of this prestellar medium, the pressure support would disappear because of their smaller surface area, and they would fall toward the center of the galaxy on nearly rectilinear orbits. However, if the gas was hot enough to support itself against the self-gravity of the entire galaxy, it was certainly hot enough to support itself against the gravity of any density fluctuation of protostellar size. It seems probable that no stars could form in such an equilibrium configuration, and some other explanation of Figure 4 is necessary.

We have plotted in Figure 6 the angular momentum,  $h$ , against the ultraviolet excess for all the stars studied here. Under the assumptions that (1) there was always axial symmetry of the mass distribution and (2) no accretion of matter onto the surface layers of any given star has occurred, then both the angular momentum and the ultraviolet excess are invariant with time and are therefore initial conditions given to the star at birth. Figure 6 shows that the oldest stars, with large ultraviolet excesses, have smaller angular momenta than those recently formed with small excesses. (It should be noted that the angular momentum for *circular* orbits at the sun's distance from the galactic center is  $h = 25 \times 10^2$  kpc km/sec, whereas stars on *elliptical* orbits passing through the sun's position have smaller values. Therefore, Fig. 6 is a different representation of the correlation shown in Fig. 4, and the explanation of one diagram will furnish the explanation of the other.)

The absence of stars in the lower left corner of Figure 6 is real, since, as discussed in Section IV, the ultraviolet excess did not enter into the selection of the stars. We therefore conclude that stars with large excess and with orbits that pass through the solar neighborhood have low angular momenta.

It is useful to ask where in the present galaxy matter exists with the same angular momentum as that of the oldest stars of highest velocity. Most of the material now near the sun is traveling in nearly circular orbits, and it is reasonable to assume that the same is true at all distances from the galactic center. Figure 7 shows the angular momenta of material moving in circular orbits at various distances from the galactic center, de-



rived from the velocity laws illustrated in Figure 1. We notice that material with the same mean angular momentum as that of the highest-velocity stars,  $h = 12 \times 10^2$  kpc km/sec, is in circular orbits at less than 5 kpc from the galactic center.

Therefore, if the galaxy in its earliest days was in dynamic equilibrium—i.e., gravitational attraction everywhere balanced by centrifugal acceleration and with circular orbits established—these oldest stars would have been formed less than 5 kpc from the center. This seems to be an unreasonable result, however, because subsequently to place these stars in their present elliptical orbits, passing through the solar neighborhood, requires

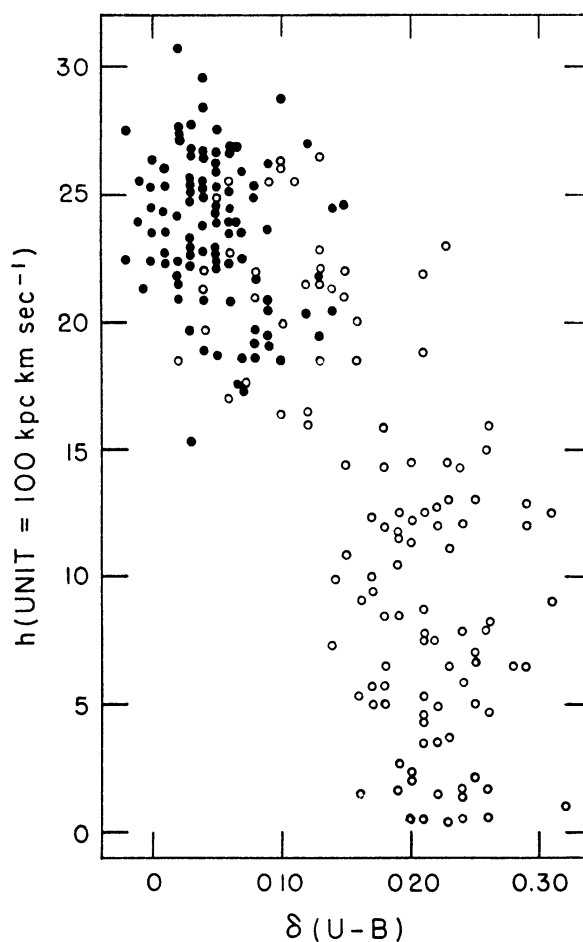


FIG. 6.—The correlation between the angular momentum,  $h$ , in units of  $10^2$  kpc km/sec and the ultra-violet excess of the stars shown in Figs. 4 and 5.

that a large amount of kinetic energy—from an unknown source—be somehow given to the stars. Velocities in excess of 100 km/sec must be imparted to change circular orbits into the present, highly elliptical orbits. *We therefore conclude that the galaxy had not settled down to its present equilibrium state at the time of first star formation but was in its initial gravitational contraction from a larger protogalaxy.* The data then require that the first stars were formed out of gas which was falling together in this initial collapse.

We can determine the rate of collapse as follows. Suppose, first, that the collapse was slow compared with the period of one galactic rotation, which is near  $2 \times 10^8$  years. A slow collapse means that the velocity of the prestellar gas in the radial direction was small compared with that in the direction of rotation. If the entire kinetic energy of the

stars was derived from the gas out of which they formed, then  $U(\text{star}) \ll V(\text{star})$ , and the initial orbital eccentricity will be small. But, by the results of Section III, the orbital eccentricities will not be changed during the subsequent slow collapse of the remaining gas, and highly eccentric orbits will never be formed, a result in contradiction with the data of Figure 4. Therefore, the rate of the collapse must have been rapid in comparison with one galactic period of  $2 \times 10^8$  years. Because there is no reason to believe that the collapse of the galaxy into a plane proceeded at a different rate than the contraction in the plane, we conclude that the time scale for the vertical contraction, involving the

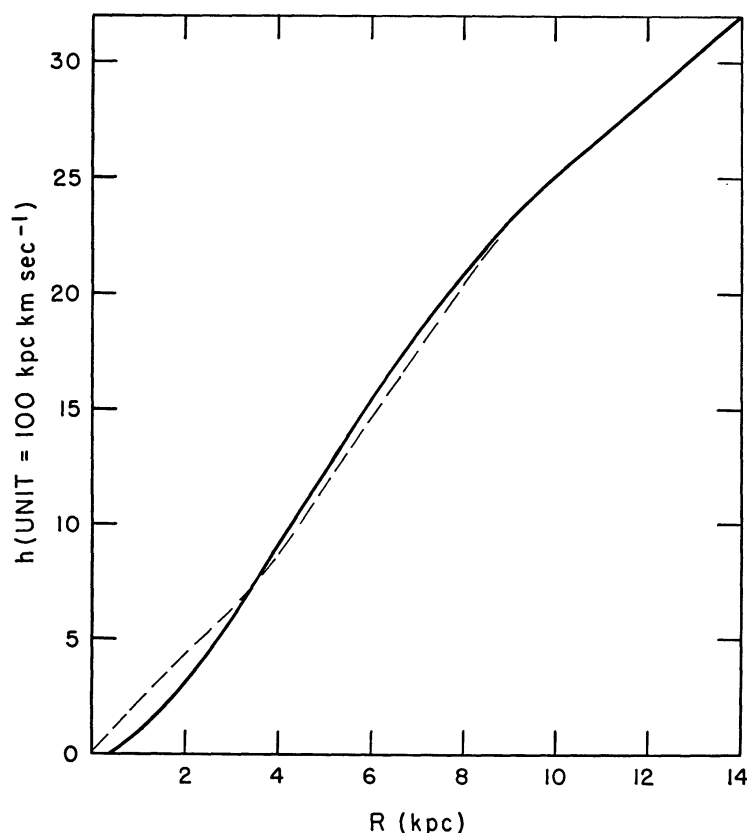


FIG. 7.—The correlation between the angular momentum,  $h$ , in units of  $10^2$  kpc km/sec and the distance from the galactic center,  $R$ , in kiloparsecs for stars in circular orbits in our model galaxy. The dashed curve corresponds with the Leiden curve in Fig. 1. The solid curve is computed from eq (6).

stars with excesses between  $\delta(U - B) = +0^m35$  and  $+0^m15$  in Figure 5, is also about  $10^8$  years. This result offers an explanation of why all the halo globular clusters for which accurate photometry is available—M3, M5, M13, M15, and M92—are so nearly of the same age. The collapse of gas out of the halo into the plane was so rapid that only about  $10^8$  years elapsed between the time when star formation started and the time when no material remained from which subsequent generations of halo stars could be formed. The available observations of halo globular clusters is neither complete nor accurate enough to determine whether or not the spread in ages is indeed as short as  $10^8$  years, but the present data do not contradict our hypothesis.

Returning to the situation in the galactic plane, we can place a lower limit on the scale of the collapse in the radial direction in the following way. The apogalactic distances

of stars with the highest eccentricity are, in several cases, larger than 50 kpc. A comparison of Figures 6 and 7 shows that the radius of circular orbits in the present, equilibrium, galaxy with the same angular momenta as the oldest stars with high eccentricity is less than 5 kpc. The history of the collapsing gas streams is very different from that of the stars because, as the streams plunge toward the galactic center on their eccentric orbits, they will collide with other streams, losing their kinetic energy, in the radial direction, by radiation, and within about  $10^8$  years they will take up circular orbits. On the other hand, the first stars, once formed, will not suffer collisions and will continue in their eccentric orbits. Therefore, we can identify second-generation stars, moving in circular orbits, and first-generation stars, with the same angular momentum but moving in highly eccentric orbits, as having been produced from the same parent gas. Because the ratio of the apogalactic distance of the first-generation stars to the radius of the circular orbit of the same angular momentum, now occupied by the second generation, is at least 10 to 1, we conclude that the present galaxy is less than one-tenth the scale of the original protogalaxy. The fact that the "collapse factor" in the plane is only 10, compared with 25 in the  $Z$ -direction, is understandable because the latter is not impeded by centrifugal acceleration as is that in the plane. Furthermore, we have no evidence against the hypothesis that the collapse discussed here is but the last stage of a collapse which began at intergalactic densities.

Figure 4 is now explained: (1) we have seen that the first-generation stars, formed *during* the galactic collapse, *now* have eccentric orbits in the fully collapsed, equilibrium galaxy; (2) second-generation stars formed after the collapse will have the nearly circular orbits in which their parent gas clouds have settled. To explain the variation of  $\delta(U - B)$ , we predict that the time elapsed between the two generations is long enough to allow the newly formed O- and B-type stars of the first generation to cook elements in their interiors, explode in supernovae outbursts, and feed the metal-enriched material back into the interstellar medium.

Further support for this general picture is obtained from the data plotted in Figure 8. Here the angular momenta are plotted against the apogalactic distances for all the stars discussed. Three groups of ultraviolet excesses are represented by closed circles, crosses, and open circles, respectively— $\delta(U - B) > 0^m21$ ,  $0^m14 < (U - B) \leq 0^m21$ , and  $\delta(U - B) < 0^m14$ . Our previous conclusion was that stars with ultraviolet excesses greater than  $0^m14$  were formed in the non-equilibrium phase of the galaxy, whereas the stars with smaller excesses were formed after the collapse had occurred and the circular velocity was that of Figure 1 and equation (6). The results shown by Figure 8 are in agreement with these conclusions if we assume that stars are formed near the apogalactica of their orbits. Stars with excesses smaller than  $+0^m14$  are well segregated from those in the other two excess groups shown in Figure 8, and, more importantly, the shape of the upper envelope of their distribution is well represented by the  $(R, h)$ -diagram of Figure 7, implying that these stars were actually formed when the galaxy had reached its equilibrium state.

One puzzling feature of Figure 6 requires comment. Stars with large angular momentum and large ultraviolet excess could exist in our model because, in the equilibrium galaxy of today, we know that gas or later-generation stars formed from it exist with circular orbits at the sun's distance from the galactic center. The angular momentum,  $h = 25 \times 10^2$  kpc km/sec, of this material at its precollapse distance of about 100 kpc could have formed stars whose angular momentum would now be same but which would be traveling in highly eccentric orbits. However, such stars are absent in Figure 6.

The same puzzling absence of stars with highly eccentric orbits and angular momenta comparable with that of the sun is shown in the  $(h, e)$ -diagram of Figure 9. This diagram also shows the interesting restrictions that are placed on the angular momenta and the eccentricity by the requirement that the orbits of the stars must pass through the solar

neighborhood to be included in our sample. The lower left region of the figure is forbidden to our sample because the apogalactica of the stars' orbits would be smaller than 10 kpc and the stars would not come as far out as the sun. In a similar manner, the upper left region of the figure is not populated because the perigalactica of the orbits of these stars are greater than 10 kpc. The vertical boundary at  $e = 1$  separates the regions of positive and negative orbital energy, and stars to the right of this boundary would escape from the galaxy.

The fact that our sample of stars does not fill the permitted area of Figure 9 can be partly explained by the presence of several unavoidable selection effects. A star spends the majority of time in the part of its orbit that contains its apogalacticum, and therefore

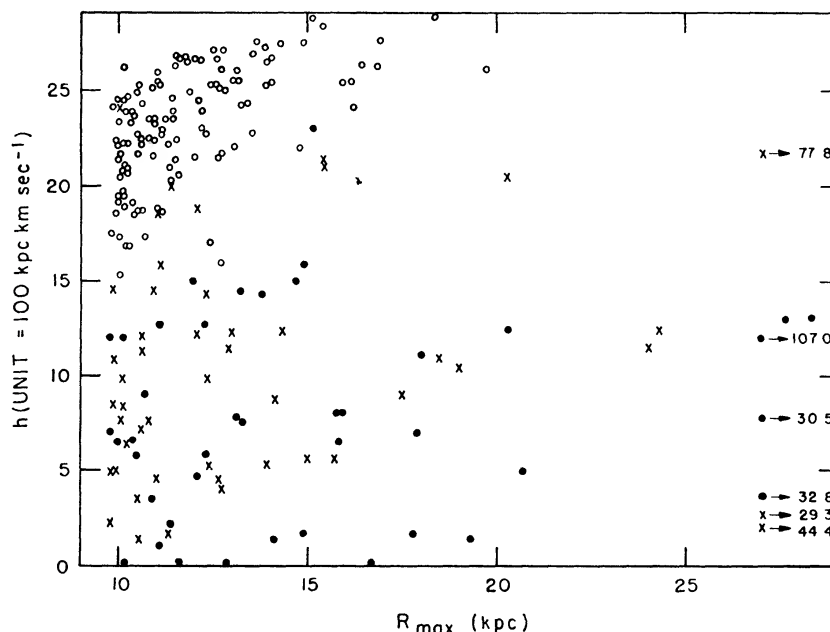


FIG. 8.—The observed correlation between the apogalactic distance and the angular momentum in the orbits of the 221 stars in our sample. Stars with ultraviolet excesses greater than  $0^m21$  are indicated by filled circles, between  $0^m14$  and  $0^m21$  by crosses, and less than  $0^m14$  by open circles. Note the well-defined upper envelope to the open circles, which follows the shape of the equilibrium curve of Fig. 7.

we are more likely to find stars whose apogalacticum is near the sun—that is, that fall along the boundary in the lower left of Figure 9. Also, the gradient of stellar density in the galactic system favors stars of small apogalactic distance, which again tends to concentrate the observed objects along the boundary in the lower left of Figure 9. The only explanation we can offer for the absence of stars in the region of angular momenta near  $25 \times 10^2$  kpc km/sec and with eccentricities greater than 0.6, in Figure 9, is that the density of the collapsing gas at the great distances (near 100 kpc) involved was insufficient to form stars until the equilibrium galaxy had been established.

## VI. SUMMARY

1. Approximately  $10^{10}$  years ago the protogalaxy started to fall together out of intergalactic material. It was either already rotating or acquired its angular momentum from the couples exerted by nearby condensations.
2. As the material fell together, condensations formed which were later to become globular clusters and globular cluster-like stars.

3. The collapse of the galaxy in the radial direction was eventually stopped by rotation, but that in the Z-direction continued, giving rise to a thin disk. With the increased density, the rate of star formation increased. In their evolution the first-generation stars enriched the remaining gas with heavy elements formed in their interiors, with the result that later generations, formed from this same material, show smaller ultraviolet excesses.

4. The gas, which must have become hot, radiated away much of the energy of collapse. At first, the gas followed the orbits of the stars that were formed from it, but the gas and the stars became separated near perigalacticum, after which, relieved of its extra energy by collisions with other gas clouds, the gas settled into circular orbits appropriate to its angular momentum and continued to produce later generations of stars that also move in nearly circular orbits. The first-generation stars, on the other hand, continue in the highly eccentric orbits produced by the original collapse.

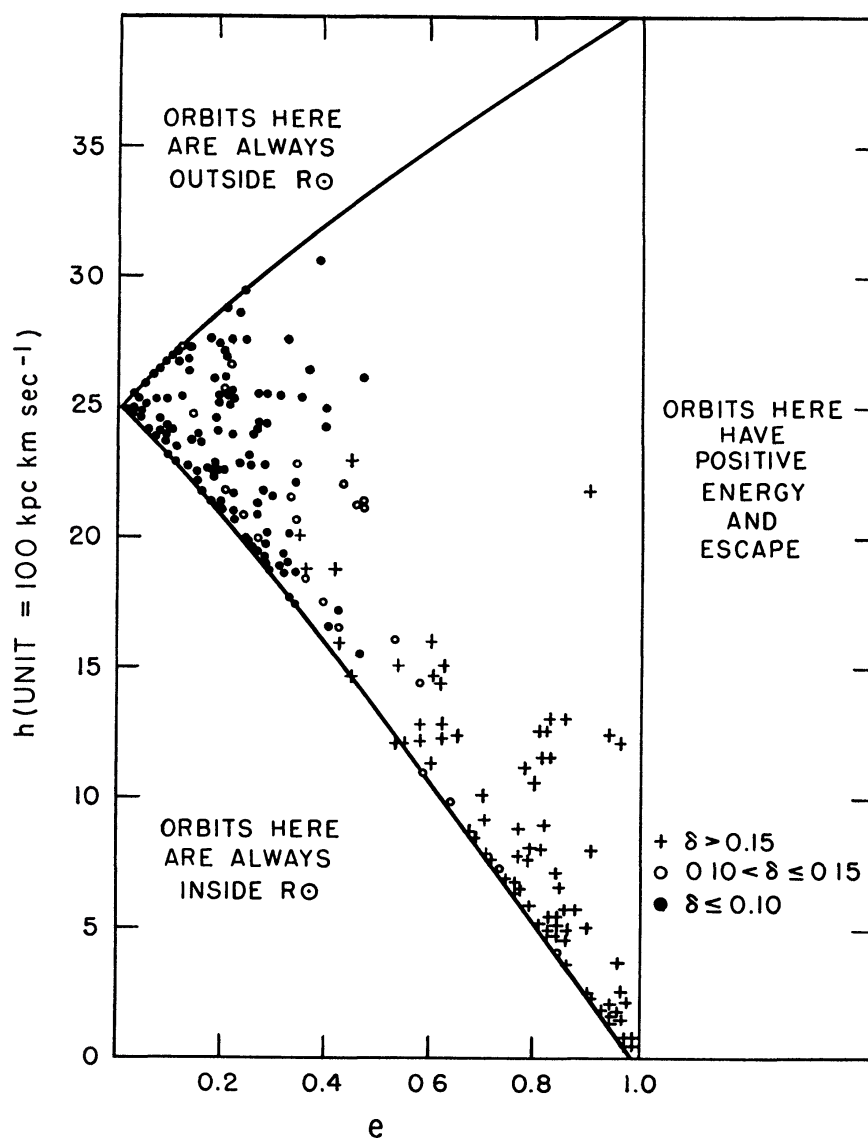


FIG 9 —The correlation between eccentricity and angular momentum. Regions expected to be free of stars represented by our sample are marked.



## REFERENCES

- Blaauw, A. 1961, *B.A.N.*, **15**, 265.  
 Eggen, O. J. 1961, *R. Obs. Bull.*, No 51.  
 ———. 1962, *R. Obs. Bull.*, in preparation.  
 Fricke, W. 1950, *A.N.*, **278**, 49.  
 Hoerner, S. von. 1955, *Zs. f. Ap.*, **35**, 255.  
 Kinman, T. D. 1959a, *M.N.*, **119**, 538.  
 ———. 1959b, *ibid.*, p. 559.  
 Lohmann, W. 1948, *Zs. f. Ap.*, **25**, 293.  
 Lynden-Bell, D. 1962, *M.N.*, **124**, 95.  
 Mayall, N. U. 1946, *Ap. J.*, **104**, 290.  
 Morgan, W. W. 1956, *Pub. A.S.P.*, **68**, 509.  
 Mestel, L. 1961, In preparation.  
 Newkirk, J. M. 1952, *Harvard Bull.* No 921, p. 15.  
 Oort, J. H. 1926, *Groningen Obs. Pub.*, No. 40.  
 Oort, J. H., and Woerkom, A. J. J. van. 1941, *B.A.N.*, **9** (No. 338), 185.  
 Preston, G. W. 1959, *Ap. J.*, **130**, 507.  
 Roman, N. G. 1954, *A.J.*, **59**, 307.  
 ———. 1955, *Ap. J. Suppl.*, No. 18, p. 195.  
 Rougoor, G. W., and Oort, J. H. 1960, *Proc. Nat. Acad. Sci.*, **46**, 1.  
 Sandage, A. R., and Eggen, O. J. 1959, *M.N.*, **119**, 278.  
 Schwarzschild, M. 1952, *A.J.*, **57**, 57.  
 Vyssotsky, A. N., and Williams, E. T. R. 1948, *Pub. McCormick Obs.*, **X**.  
 Wallerstein, G. 1962, *Ap. J. Suppl.*, No. 61, p. 407.  
 Woolley, R. v.d. R. 1958, *M.N.*, **118**, 45.  
 Yasuda, H. 1961, *Ann. Tokyo Obs.* 2d ser., Vol. 7, No 1.